Glyphosate exposure modulates the expression of c-jun, ikkb and NF-κappaβ mRNA expression in skeletal muscle of male Wistar rats.

Sangaraju Soumya Sri, Kavitha S*, Selvaraj J, V Vishnupriya, Gayathri R

Department of Biochemistry, Saveetha Institute of Medical and Technical Sciences, Chennai, India

Abstract

Diabetes is a metabolic disorder and Nuclear Factor κappaβ (NF-κβ) plays a key role in the pathogenesis of diabetes. Glyphosate is a herbicide and crop desiccant, it is used to kill weeds and grasses that compete with crops. c-jun is an important component of AP-1 it gives an early response transcriptional factor that regulates the expression of a diverse range of genes. To study the effect of glyphosate exposure on the expression of c-jun, IKKB, and NF-kappaB mRNA expression in skeletal muscle of male Wistar rat. The present study suggests that glyphosate exposure to animals caused a significant increase in the expression of inflammatory signaling molecules in skeletal muscle indicating that glyphosate induces diabetes by activating inflammatory signaling in a dose-dependent manner.

Keywords: Diabetes, Skeletal muscle, Inflammation, Glyphosate, c-Jun, NF-κappaβ, Innovative technology, Novel method

Accepted on November 03, 2021

Introduction

Glyphosate is a nonspecific herbicide widely used in the name of 'Roundup'. Glyphosate is the only herbicide to target the enzyme 5-enolpyruvyl-3-shikimate phosphate synthase. Glyphosate phloem-mobile features and slow action in killing weeds allow the herbicide to flow throughout the plant to kill all meristems, making it effective for perennial weed control. Glyphosate is considered the best and non-selective herbicide before the introduction of Glyphosate-Resistant Crops (GRCs). However, the introduction of GRCs greatly increased its use in those countries approving their cultivation. c-Jun is an important component of AP-1 which gives a quick response to transcriptional factor that causes the expression of a different range of genes [1-4]. Studies have shown that c-Jun is necessary for the formation of the epidermal leading edge by controlling an EGF autocrine loop and c-Jun-deficient fibroblasts have been reported to inhibit the proliferation of co-cultured keratinocytes [5-7].

As a transcription factor, Nuclear factor κappaβ (NF-κβ) is one of the cross-talk points of various signal transduction pathways, which plays a crucial role in the regulation of transcription and the expression of more genes involved in inflammatory responses [8-10]. A better understanding of the mechanisms involved in NF-κβ regulation and its modulation may provide new tools to improve the treatment of diabetes-induced renal diseases with a better understanding of its pathophysiological approach [11-13].

The NF-κappaβ is a DNA binding protein factor that is involved in the transcription of different proinflammatory and inflammatory molecules like cytokines, chemokines, Cell Adhesion Molecules (CAM) and different enzymes [14-16]. NF-κappaβ is an evolutionarily conserved protein from the Rel family found in all cell types [17]. The NF-κappaβ is activated *via* two pathways *viz.* canonical pathway and non-canonical pathway [18]. In canonical pathway when a signal is transduced, NEMO-containing IKK complexes are activated and induce phosphorylation of IKK complex *via* ubiquitination leading to release of NF-κβ dimers [19]. Inhibition of NF-κappaβ activation may provide treatment options in Diabetic neuropathy by inhibiting transcription of genes and blocking inflammatory processes. A few researchers studied the effect of NF-κβ inhibition on Diabetic neuropathy [20-22]. Various natural and synthetic NF-κappaβ inhibitors have been studied for their protective effect in diabetic neuropathy. The effect of glyphosate on the expression of Ikκβ, c-jun, NF-κβ, was not studied so far on male Wistar rats. Glyphosate raises the environmental threat and also public health concerns, hence we investigated the effects of glyphosate on the m-RNA expressions. Our team has extensive knowledge and research experience that has translate into high quality publications [23-40].

The study aims to assess the impact of glyphosate exposure on the increased expression of c-JUN, IKKB, and NF-κappaβ mRNA in skeletal muscle of male Wistar rats.

Materials and Methods

Chemicals

All chemicals and reagents used in this study were purchased from Sigma Chemical Company St. Louis, MO, USA; Invitrogen, USA; Eurofins Genomics India Pvt Ltd, Bangalore, India; New England Biolabs (NEB), USA; Promega, USA. Glyphosate was procured from Sigma Chemical Company St. Louis, MO, USA; Total RNA isolation reagent (TRIR) was purchased from Invitrogen, USA. The reverse-transcriptase enzyme (MMuLv) was purchased from Genet Bio, South Korea purchased from Promega, USA.

Animals

The present experimental study was approved by the institutional animal ethics committee (IAEC no.: BRULAC/SDCH/SIMATS/IAEC/02-2019/015). Adult male Wistar albino rats, weighing 180–200 g, were obtained and maintained in clean propylene cages at the Biomedical Research Unit and Laboratory Animal Centre (BRULAC), Saveetha dental college and hospitals, Saveetha University, India) in an air-conditioned animal house, fed with standard rat pelleted diet (Lipton India Ltd., Mumbai, India), and clean drinking water was made available ad libitum. Rats were divided into 4 groups, each consisting of 6 animals.

Experimental design

Group 1: Normal control.

Group 2: Glyphosate treated (glyphosate was dissolved in water at a dose of 50

mg/kg b.wt/day at 8 am, orally for 16 weeks.

Group 3: Glyphosate treated (glyphosate was dissolved in water at a dose of 100

mg/kg b.wt/day at 8 am, orally for 16 weeks.

Group 4: Glyphosate treated (glyphosate was dissolved in water at a dose of 250

mg/kg b.wt/day at 8 am, orally for 16 weeks.

At the end of the treatment, animals were anesthetized with sodium thiopentone (40 mg/kg b.wt), blood was collected through the cardiac puncture, sera were separated and stored at −80°C, and 20 ml of isotonic sodium chloride solution was perfused through the left ventricle to clear blood from the organs. Skeletal tissues from control and experimental animals were immediately dissected out and used for assessing the various parameters.

Assessment of Fasting Blood Glucose (FBG)

After the overnight fasting, the blood glucose was estimated using On-Call Plus blood glucose test strips (ACON Laboratories Inc., USA). From the rat tail tip, the blood was collected and results were expressed as mg/dl.

Oral Glucose Tolerance Test (OGTT)

For oral glucose tolerance tests, animals fasted overnight. After giving the oral glucose load (10 ml/kg; 50% w/v). blood glucose level was estimated at various time periods (60, 120, and 180 min) by using On-Call Plus blood glucose test strips. Before giving a glucose load, the value of blood glucose is considered as 0 min value. Results were marked as mg/dl.

Isolation of total RNA

Total RNA was isolated from control and experimental samples using total RNA isolation reagent (TRIR) kit. Briefly, 100 mg fresh tissue was homogenized with 1 ml TRIR and the homogenate was transferred immediately to a microfuge tube and kept at -80°C for 60 min to permit the complete dissociation of nucleoprotein complexes. Then, 0.2 ml of chloroform was added, vortexed for 1 min, and placed on ice at 4°C for 5 min. The homogenates were centrifuged at 12,000 x g for 15 min at 4°C. The aqueous phase was carefully transferred to a fresh microfuge tube and an equal volume of isopropanol was added, vortexed for 15 sec, and placed on ice at 4°C for 10 min. The samples were centrifuged at 12,000 xg for 10 min at 4°C. The supernatant was discarded and RNA pellet was washed with 1 ml of 75% ethanol by vortexing and subsequent centrifugation for 5 min at 7,500 xg (4°C). The supernatant was removed and RNA pellets were mixed with 50 µl of autoclaved Milli-Q water and dissolved by heating in a water bath for 10 min at 60°C.

Quantification of RNA

Diluted RNA samples were quantified spectrophotometrically by measuring the absorbance (A) at 260/280 nm. 40 µg of RNA in 1 ml gives one absorbance at 260 nm. Therefore, the concentration of RNA in the given sample can be determined by multiplying its A260 by 40 and the dilution factor. The purity of RNA preparation can be calculated using the ratio between its absorbance at 260 and 280 nm. A ratio of absorbance at 260/280 nm >1.8 is generally considered as good quality RNA. The purity of RNA obtained was 1.8.

Reverse Transcriptase–Polymerase Chain Reaction (RT–PCR)

RT-PCR is an approach for converting and amplifying a single-stranded RNA template to yield abundant double-stranded DNA products. 1. First-strand reaction: Complementary DNA (cDNA) is made from the mRNA template using Oligo dT, dNTPs and reverse transcriptase. 2. Second strand reaction: After the reverse transcriptase reaction is complete, standard PCR (called the “second strand reaction”) is initiated. Principle RT-PCR is a method used to amplify cDNA copies of RNA. It is the enzymatic conversion of mRNA into a single cDNA template. A specific oligodeoxynucleotide primer hybridizes to the mRNA and is then extended by an RNA-dependent DNA polymerase to create a cDNA copy. First-strand DNA synthesis The RT kit was purchased from Eurogentec (Seraing, Belgium). Reagents 1. 10X RT buffer: One vial containing 1.4 ml of 10X RT buffer. 2. EuroScript reverse transcriptase: One tube containing 75 µl of Moloney murine leukemia virus reverse transcriptase (3750 U at 50 U/µl).

Quantitative real-time PCR principle

The purpose of a Polymerase Chain Reaction (PCR) is to make a huge number of copies of a gene. There are three major steps in a PCR, which are as follows: Denaturation at 94°C for 3 min: During the denaturation at 94°C for 2-5 min, the double-strand melts open to single-stranded DNA, all enzymatic reactions stop. Annealing at 54°C-65°C for 30 sec: Ionic bonds are constantly formed and broken between primer and the single-stranded template to ensure the extension process. Extension at 72°C for 30 sec: Primers that are in positions with no exact match get loose again (because of the higher temperature) and don't give an extension of the fragment. The

bases (complementary to the template) are coupled to the primer on the 3' side (the polymerase adds dNTP from 5' to 3', reading the template from 3' to 5' side; bases are added complementary to the template). Because both strands are copied during PCR, there is an exponential increase in the number of copies of the gene.

Reagents

1. 2X Reaction buffer: The PCR master mix kit was purchased from Takara

Bio Inc. Japan. Contains TaKaRa Ex Taq HS (a hot-start PCR enzyme) dNTP

Mixture, Mg2+, Tli RNase H (a heat-resistant RNase H that minimizes PCR

inhibition by residual mRNA), and SYBR Green I.

2. Forward primer (10 µM)

3. Reverse primer (10 µM)

4. cDNA- Template.

5. Autoclaved milli Q water.

6. Primers.

The following gene-specific oligonucleotide primers were used.

Rat IKKB

FW- 5' -AGCTCTGGAACCTCCTGAAGA – 3'

RW- 5' – AGCTCCAGTCTAGGGTCGTGA – 3'

Rat c-JUN

FW: 5'-AGACGCTTGAGTTGAGAGCC-3'

RW: 5'-CTTCAGTGTGCGGCTTAGGA-3'

Rat-Nfκβ

FW: 5'-GCTTTGCAAACCTGG GAATA-3'

RW: 5'-CAAGGTCAGAAT GCACCAGA-3'

Rat β-actin

FW – 5'- TACAGCTTCACCACCACAGC - 3'

RW– 5'- TCTCCAGGGAGGAAGAGGAT - 3'

Procedure

Real-Time PCR was carried out on the CFX 96 Real-Time system (Bio-Rad). The reaction mix (10 µl) was prepared by adding 5 µl of 2X reaction buffer, 0.1 µl of sense and antisense primer, 1 µl of cDNA, and 3.8 µl of sterile water. The thermal cycler protocol was as follows: Initial denaturation at 95°C for 3 min, followed by 40 cycles of PCR, denaturation at 95°C for 10 sec, annealing at 60°C for 20 sec and extension at 72°C for 20 sec. All reactions were performed in triplicate along with No Template Control (NTC). Melt curve analysis was performed using the thermal cycling programmed at 50°C-95°C for each sample to determine the presence of multiple amplicons, non-specific products, and contaminants.

The results were analyzed using CFX 96 Real-Time system software (Bio-Rad). As an invariant control, the present study used rat β-actin.

Statistical Analysis

The triplicate analysis results of the experiments performed on control and treated rats were expressed as mean standard deviation. Results were analyzed statistically by a one-way Analysis of Variance (ANOVA) and significant differences between the mean values were measured using Duncan's multiple range test using graph pad prism version 5. The Results with the $p<0.05$ level were considered to be statistically significant.

Results

Due to exposure to glyphosate, there was an increase in the c-JUN m- RNA expression in the animals exposed to glyphosate compared to the control rats. Compared to controlled rats' value of c-jun/beta-actin, group 1 rats showed a decreased expression of approximately 1.0 c-JUN, while group 2 and 3 showed increased expression to approximately 1.5 c-JUN/beta-actin. This signifies a significantly increased expression of c-jun in glyphosate exposed groups of rats. The greater the exposure was an impaired expression though not necessarily consistent. Similarly, there was an increase in the expression of IKKB m-RNA in the rats exposed to glyphosate compared to controlled rats. Compared to controlled rats' value of ikκβ/beta-actin, group 1 rats showed a decreased expression of approximately 1.2 IKKB, while group 2 and 3 showed increased expression to approximately 1.7 ikκβ/beta-actin.

This signifies a significantly increased expression of IK in KB glyphosate-exposed groups of rats. The greater the exposure the greater was the impaired expression though not necessarily consistent. The same goes with NFκβ. There was a significant increase in the expression of NFκβ m-RNA in the rats exposed to glyphosate compared to controlled rats.

Compared to controlled rats' value of ikκβ/beta-actin, group 1 rats showed a decreased expression of approximately 1.3 NFκβ while group 2 and 3 showed increased expression to approximately 1.6 NFκβ/beta-actin.

This signifies a significantly increased expression of NFκβ in glyphosate-exposed groups of rats. The
greater the exposure the greater was the impaired expression though not necessarily consistent (Figures 1-3).

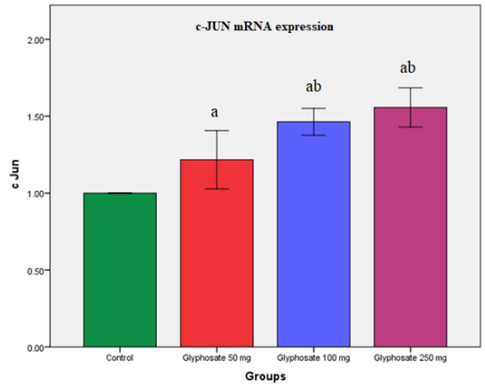

Figure 1. *Impact of glyphosate on the mRNA expression of c-JUN in adult male rats X-axis represents the amount of glyphosate which was exposed to the rats. Y-axis represents the fold change in the C-JUN mRNA molecule expression in experimental rats in comparison to control rats. Green colour represents the controlled rats, Dark red colour represents group 1 rats exposure to about 50 mg glyphosate, Dark blue colour represents group 2 rats exposure to about 100 mg of glyphosate, Pink colour represents group 3 rats exposure to about 250 mg of glyphosate. The mRNA expressions were assessed by Real-Time -PCR. Each bar represents mean SEM (n=6). Significance at p<0.05, a: Significantly different from the control group. b: Significantly different from diabetic control.*

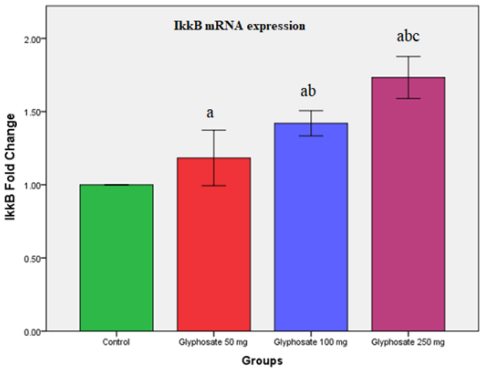

Figure 2. *Impact glyphosate on the mRNA expression of IKκappaβ in adult male rats. The X-axis represents the amount of glyphosate which was exposed to the rats. Y-axis represents the fold change in the IKKB mRNA molecule expression in experimental rats in comparison to control rats. Green colour represents the controlled rats, dark red colour represents group 1 rats exposure to about 50 mg glyphosate, dark blue colour represents group 2 rats exposure to about 100 mg of glyphosate, pink colour represents group 3 rats exposure to about 250 mg of glyphosate. The mRNA expressions were assessed by Real-Time-PCR. Each bar represents mean SEM (n=6). Significance at p<0.05, a: Significantly different from the control group. b: Significantly different from diabetic control.*

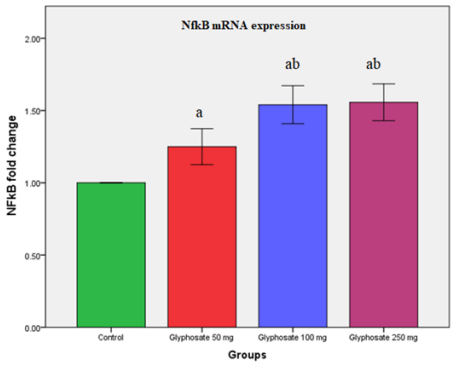

Figure 3. *Impact of glyphosate on the mRNA expression of NF-κappaβ in adult male rats. The X-axis represents the amount of glyphosate which was exposed to the rats. Y-axis represents the fold change in the NFκβ mRNA molecule expression in experimental rats in comparison to control rats. Green colour represents the controlled rats. Dark red colour represents group 1 rats exposure to about 50 mg glyphosate. Dark blue colour represents group 2 rats exposure to about 100 mg of glyphosate. Pink colour represents group 3 rats exposure to about 250 mg of glyphosate. The mRNA expressions were assessed by Real-Time-PCR. Each bar represents mean SEM (n=6). Significance at p<0.05, a: Significantly different from the control group. b: Significantly different from diabetic control.*

Discussion

The present study suggests that glyphosate exposure to experimental animals caused a significant increase in the expression of inflammatory signalling molecules in skeletal muscle indicating that glyphosate induces diabetes by activating inflammatory signalling in a dose-dependent manner. By the present study, few clinical studies have shown that a considerable amount of glyphosate concentration was found to be measured in diabetic patients. This study indicates that there is a relationship between glyphosate exposure and the development of diabetes in experimental animals.

A previous study done by Khan et al. has suggested that chronic exposure of experimental animals to metal toxins such as Arsenic has resulted in diabetes. The study was done by Nadeem et al 2021, strongly suggests that NF-Kappaβ acts as a central inflammation pathway that responds to various immune receptors. Inflammations are taken as a primary marker for many non-pathological disorders like diabetes and other heart-related ailments. In this current study, there was an increased expression of inflammatory markers in the experimental animals after the prolonged exposure to glyphosate. From the results, it is evident that prolonged exposure to non-specific herbicide may result in the accumulation of free radicals and thus there is a concomitant increase in inflammation. Further, studies have to be conducted to elucidate the relation of glyphosate with increased free radical production. A study done by Broude et al. has concluded that results c-Jun was upregulated substantially in DRG neurons following a peripheral axotomy, but following a central axotomy, only 18%

of the neurons expressed c-Jun. Following dorsal rhizotomy and transplantation, however, c-Jun expression was upregulated dramatically; under those experimental conditions, 63% of the DRG neurons were c-Jun-positive. These data indicate that c-Jun expression may be related to successful regenerative growth following both PNS and CNS lesions. A study done by Abeel et al. have concluded that Ikκβ on long exposure to glyphosate may lead to detrimental effects.

Limitations of the present study are this study was done within a limited period and also this study was done with just three varied doses of glyphosate. If this study was conducted using more varied doses then it would have helped us with obtaining more accurate side effects on the expressions. In the future, further studies need to be done to take care of the treatment modalities and other side effects created by the long-term exposure of the non-specific herbicide.

Conclusion

It is concluded from the present findings that chronic exposure to glyphosate may induce the expression of inflammatory signaling molecules like Ikκβ /C-JUN/NF-κappaβ. Since inflammation is the root cause of various disorders, further studies have to be done to prove the detrimental effects of long-term exposure to glyphosate.

Acknowledgement

The authors would like to thank Saveetha dental college and hospitals, Saveetha Institute of medical and technical sciences, Saveetha University for providing research laboratory facilities to carry out the study.

Source of Funding

The present study was supported by the following agencies: Saveetha Institute of Medical and Technical Sciences (SIMATS), Saveetha dental college, Saveetha University, Sreenadh dental clinic, Tirupathi.

Statement of Conflict of Interest

The author declares that there is no conflict of interest in the present study.

References

1. Babu S, Jayaraman S. An update on β-sitosterol: A potential herbal nutraceutical for diabetic management. Biomed Pharmacother. 2020;131:110702.
2. Barma, M D, Muthupandiyan I, Samuel SR, et al. Inhibition of *Streptococcus mutans,* antioxidant property and cytotoxicity of novel nano-zinc oxide varnish. Arch Oral Biol. 2021;126:105132.
3. Chen F, Tang Y, Sun Y, et al. 6-shogaol, a active constiuents of ginger prevents UVB radiation mediated inflammation and oxidative stress through modulating NrF2 signaling in human epidermal keratinocytes (HaCaT cells)', J Photochem Photobiol B. 2019;197:111518.
4. Gothai S, Muniandy K, Gnanaraj C, et al. Pharmacological insights into antioxidants against colorectal cancer: A detailed review of the possible mechanisms. Biomed Pharmacother. 2018;107:1514–1522.
5. Han X, Jiang X, Guo L, et al. Anticarcinogenic potential of gold nanoparticles synthesized from *Trichosanthes kirilowii* in colon cancer cells through the induction of apoptotic pathway. Artif Cells Nanomed Biotechnol. 2019;47(1): 3577–3584.
6. Kadanakuppe S, Hiremath S. Social and behavioural factors associated with dental caries experience among adolescent school children in Bengaluru city, India. J Adv Med. 2016;14(1):1–10.
7. Li Z, Veeraraghavan VP, Mohan SK, et al. Apoptotic induction and anti-metastatic activity of eugenol encapsulated chitosan nanopolymer on rat glioma C6 cells *via* alleviating the MMP signaling pathway. J Photochem Photobiol B. 2020;203:111773.
8. Malaikolundhan H, Mookkan G, Krishnamoorthi G, et al. Anticarcinogenic effect of gold nanoparticles synthesized from *Albizia lebbeck* on HCT-116 colon cancer cell lines. Artif Cells Nanomed Biotechnol. 2020;48(1):1206–1213.
9. Mickymaray S, Alfaiz FA, Paramasivam A, et al. Rhaponticin suppresses osteosarcoma through the inhibition of PI3K-Akt-mTOR pathway. Saudi J Biol Sci. 2021;28(7):3641–3649.
10. Rajendran P, Alzahrani AM, Rengarajan T, et al. Consumption of reused vegetable oil intensifies BRCA1 mutations. Crit Rev Food Sci Nutr. 2020;1–8.
11. Samuel SR. Can 5-year-olds sensibly self-report the impact of developmental enamel defects on their quality of life? Int J Paediatr Dent. 2021;31(2):285–286.
12. Samuel SR, Kuduruthullah S, Khair AMB, et al. Dental pain, parental SARS-CoV-2 fear and distress on quality of life of 2 to 6 year-old children during COVID-19. Int J Paediatr Dent. 2021;31(3):436–441.
13. Sathya S, Ragul V, Veeraraghavan VP, et al. An *in vitro* study on hexavalent chromium [Cr(VI)] remediation using iron oxide nanoparticles based beads. Environ Nanotechnol Monit. 2020;14:100333.
14. Tang Y, Rajendran P, Veeraraghavan VP, et al. Osteogenic differentiation and mineralization potential of zinc oxide nanoparticles from *Scutellaria baicalensis* on human osteoblast-like MG-63 cells. Mater Sci Eng C. 2021;119(3): 111656.
15. Teja KV, Ramesh S. Is a filled lateral canal-A sign of superiority? J Dent Sci. 2020;15(4):562–563.
16. Veeraraghavan VP, Hussain S, Balakrishna JP, et al. A comprehensive and critical review on ethnopharmacological importance of desert truffles: *Terfezia claveryi, Terfezia boudieri,* and *Tirmania nivea*. Food Rev Int. 2010;1–20.
17. Veeraraghavan VP, Periadurai ND, Karunakaran T, et al. Green synthesis of silver nanoparticles from aqueous extract of *Scutellaria barbata* and coating on the cotton fabric for antimicrobial applications and wound healing

activity in fibroblast cells (L929). Saudi J Biol Sci. 2021;28(7):3633–3640.

18. Wu F, Zhu J, Li G, et al. Biologically synthesized green gold nanoparticles from *Siberian ginseng* induce growth-inhibitory effect on melanoma cells (B16). Artif Cells Nanomed Biotechnol. 2019 Dec;47(1):3297–305.
19. Yang Z, Pu M, Dong X, et al. Piperine loaded zinc oxide nanocomposite inhibits the PI3K/AKT/mTOR signaling pathway *via* attenuating the development of gastric carcinoma: *In vitro* and *in vivo* studies. Arab J Chem. 2020;13(5):5501–5516.
20. Yin Z, Yang Y, Guo T, et al. Potential chemotherapeutic effect of betalain against human non-small cell lung cancer through PI3K/Akt/mTOR signaling pathway. Environ Toxicol. 2021;36(6):1011–1020.
21. Ansari MY, Ahmad N, Voleti S, et al. Mitochondrial dysfunction triggers a catabolic response in chondrocytes *via* ROS-mediated activation of the JNK/AP1 pathway. J Cell Sci. 2020;133(22):247353.
22. Baker RG, Hayden MS, Ghosh S. NF-κB, inflammation, and metabolic disease. Cell Metab. 2011;13(1):11–22.
23. Chen L, Zhang J, Zhang Y, et al. Improvement of inflammatory responses associated with NF-κB pathway in kidneys from diabetic rats. Inflamm Res. 2008;57(5):199–204.
24. Chou CW. A study of the expression of NF-κβ in central nervous system of rats with neuropathic pain. 2017.
25. Davies CC, Chakraborty A, Diefenbacher ME, et al. Arginine methylation of the c-Jun coactivator RACO-1 is required for c-Jun/AP-1 activation. EMBO J. 2013;32(11): 1556–1567.
26. Duke SO, Powles SB. Glyphosate: a once-in-a-century herbicide. Pest Manag Sci. 2008;64(4):319–325.
27. Karin, M, Ben-Neriah Y. Phosphorylation meets ubiquitination: The control of NF-κB activity. Annu Rev Immunol. 2000;18:621–663.
28. Kavitha M, Ramanathan S, Narayanan R, et al. Solution combustion synthesis and characterization of strontium substituted hydroxyapatite nanocrystals. Powder Technology. 2014:253:129–137.
29. Khan F, Momtaz S, Niaz K, et al. Epigenetic mechanisms underlying the toxic effects associated with arsenic exposure and the development of diabetes. Food Chem Toxico. 2017;107:406–417.
30. Lawrence, T. The Nuclear Factor NF- B Pathway in Inflammation. Cold Spring Harb Perspect Biol. 2009;1(6): 001651.
31. Lekha L, Raja KK, Rajagopal G, et al. Synthesis, spectroscopic characterization and antibacterial studies of lanthanide (III) Schiff base complexes containing N, O donor atoms. J Mol Struc. 2014;307–313.
32. Maia FCC, Porto RB, Magalhães LR, et al. Cardiovascular damage associated with subchronic exposure to the glyphosate herbicide in Wistar rats. Toxicol Ind Health. 2021;37(4):210-218.
33. Nadeem A, Ahmad SF, Al-Harbi NO, et al. Aggravation of autism-like behavior in BTBR T+tf/J mice by environmental pollutant, di-(2-ethylhexyl) phthalate: Role of nuclear factor erythroid 2-related factor 2 and oxidative enzymes in innate immune cells and cerebellum. Int Immunopharmacol. 2021;91:107323.
34. Neelakantan P, Cheng CQ, Mohanraj R, et al. Antibiofilm activity of three irrigation protocols activated by ultrasonic, diode laser or Er:YAG laser *in vitro*. Int Endod J. 2015;48(6):602–610.
35. Riedel M, Berthelsen MF, Cai H, et al. *In vivo* CRISPR inactivation of Fos promotes prostate cancer progression by altering the associated AP-1 subunit Jun. Oncogene. 2021;40(13):2437-2447.
36. Sahu D, Kannan GM, Vijayaraghavan R. Size-dependent effect of zinc oxide on toxicity and inflammatory potential of human monocytes. J Toxicol Environ Health A. 2014;77(4):177–191.
37. Suryavanshi SV, Kulkarni YA. NF-κβ: A potential target in the management of vascular complications of diabetes. Front Pharmacol. 2014;8:798.
38. Szabowski A, Szabowski MN, Andrecht S, et al. c-Jun and JunB antagonistically control cytokine-regulated mesenchymal–epidermal interaction in skin. Cell. 2000;103(5):745–755.
39. Vijayakumar GNS, Srinivasan D, Rathnakumari M. et al. Synthesis of electrospun ZnO/CuO nanocomposite fibers and their dielectric and non-linear optic studies. J Alloys Compounds. 2010;507(1):225–229.
40. Wang L, Jia Z, Wang B, et al. Berberine inhibits liver damage in rats with non-alcoholic fatty liver disease by regulating TLR4/MyD88/NF-κB pathway. Turk J Gastroenterol. 2020;31(12):902-909.

*Corresponding to:

Kavitha S

Department of Biochemistry

Saveetha Institute of Medical and Technical Sciences

Chennai

India

E-mail: kavithas.sdc@saveetha.com